의학석사학위논문

Comparison of genomic characteristics of synchronous intracranial meningiomas of different histological grade

서로 다른 조직학적 단계의 동시성 뇌수막종의 유전체 변이 특성 비교

2017 년 2 월

서울대학교 대학원

의학과 신경외과학 석사과정

Tamrin Chowdhury

A Thesis of Master's Degree

Comparison of genomic characteristics of synchronous intracranial meningiomas of different histological grade

서로 다른 조직학적 단계의 동시성 뇌수막종의 유전체 변이 특성 비교

February 2017

Graduate School of Medicine
Seoul National University
Neurosurgery

Tamrin Chowdhury

Comparison of genomic characteristics of synchronous intracranial meningiomas of different histological grade

지도 교수 이상형

이 논문을 의학석사학위논문으로 제출함
2016 년 10월

서울대학교 대학원

의학과 신경외과학 석사전공
Tamrin Chowdhury

Tamrin Chowdhury의 의학석사 학위논문을 인준함
2016 년 12월

위 원 장 _____ (인)
부위원장 _____ (인)
위 원 _____ (인)

Abstract

Comparison of genomic characteristics of synchronous intracranial meningiomas of different histological grade

Tamrin Chowdhury
Neurosurgery
College of Medicine
Seoul National University

Meningioma is the most common tumor of the central nervous system. Although several genetic studies of meningioma reveals various significant mutation related to meningioma development but still further studies are needed for confirming specific mutations. Here whole exome study was done on two meningioma samples of different histological grade obtained from a patient with multiple meningioma. This study shows that the each meningioma shows distinct tumor mutation despite from the same patient. Also both the meningioma shows distinct separate relations with different pathways. The common genetic abnormal incidence was the loss of Heterozygosity of the chromosome 22 in both tumors which maybe the cause of the tumor development and the subsequent mutations

plays a role in progression towards different grades.

Keyword: Meningioma, Development, Progression, Next generation sequencing

Student Number: 2015-22194

Table Of Contents

List of Tables

List of Figures

Chapter 1. Introduction

1.1. Study Background

Meningioma is the most common tumor of the central nervous system (CNS) which accounts for more than 30% of all CNS tumors in the United States.[1] Korea has the similar ratio of meningioma incidence covering more than 32% of all CNS.[2, 3] Recent updates on WHO classification of tumors of CNS in 2016 held on to three-tiered grading system of meningioma based on the aggressiveness of microscopic features, save for more strict definition of brain invasion for atypical meningioma (grade II).[4] The cytogenetic alterations, such as monosomy 22, has long been recognized as one of the important genomic characteristics in meningioma.[5] However, it was not until the recent years that started to apprehend the genomic landscape of meningioma tumorigenesis and progression by the extensive genome profiling studies. Not only the loss of chromosome 22q and *NF2* gene mutations are the most consistent driver alterations, but also several other driver mutations such as *KLF4, TRAF7, SMO*, and *AKT1* were found in non-*NF2* meningioma.[6-8] In spite of extended knowledge of genomic alterations in meningioma, there are still controversies that the meningiomas are monoclonal or polyclonal tumors.[9, 10] Moreover, the evidence of clonal origin of multiple meningioma is disputed by the hypotheses of genetic mosaicism or germline mutations.[11] Therefore, it is important to investigate the genomic alterations in synchronous tumors from the same patient, which can minimize the genetic noise to identify efficiently the driver genes of tumorigenesis and the clonality in meningiomas. We explored into a rare case of sporadic

synchronous meningiomas with different histological grade to profile the genetic alterations, in search of genes responsible for the meningioma tumorigenesis and progression as well as their clonality.

1.2. Purpose of Research

The purpose of the study was to investigate the genomic and clonal origin of synchronous meningiomas, and their evolution into different histological grades and types. The results drawn from the present study is expected to help identifying clues for meningiomagenesis in general.

Chapter 2. Materials and Methods

2.1 Case History

A 59-year-old female patient was presented with headache and left side motor weakness worsening in 3 months.

Magnetic resonance images (MRI) revealed about 5.5X4.7 cm sized well-enhancing solid and cystic mass in right fronto-parietal lobes, and about 2.2X1.6 cm sized enhancing mass in left parietal lobe (Figure 1). The preoperative impression was bilateral convexity meningiomas with possible malignant histology for the right side mass.

Both tumors were totally resected after craniotomies in one session. Fluorescence-guided surgery using 5-ALA was done, and both tumors were positive for red fluorescence (Figure 2A and 2B). Tumor tissues were preserved in liquid nitrogen just after the resection for the study, and part of tissues were sent to the pathology department for histological diagnosis. The histological diagnosis of the right sided tumor was atypical meningioma of meningothelial type and WHO grade II (AMNG) based on its high proliferative index of Ki-67 11.64% (Figure 3A). On the other hand, the left sided tumor was diagnosed as a psammomatous type of meningioma, WHO grade I (BMNG). There was extensive calcification with scanty evidence of mitotic cells in this tumor (Figure 3B).

The patient showed no postoperative neurological deficit after surgery and was discharged with the advice of adjuvant radiotherapy.

Figure 1. Magnetic resonance image of coronal view showing bilateral synchronous tumor based on dura mater. Right side mass shows heterogeneous enhancement of solid and cystic nature with peritumoral edema implying higher grade histology, while left side mass shows homogeneous well-demarcated solid nature typical of low grade meningioma

Figure 2A. Surgical view of right sided mass. Soft, fragile mass with cystic fluid was in strong red fluorescence which distinguishes from normal brain.

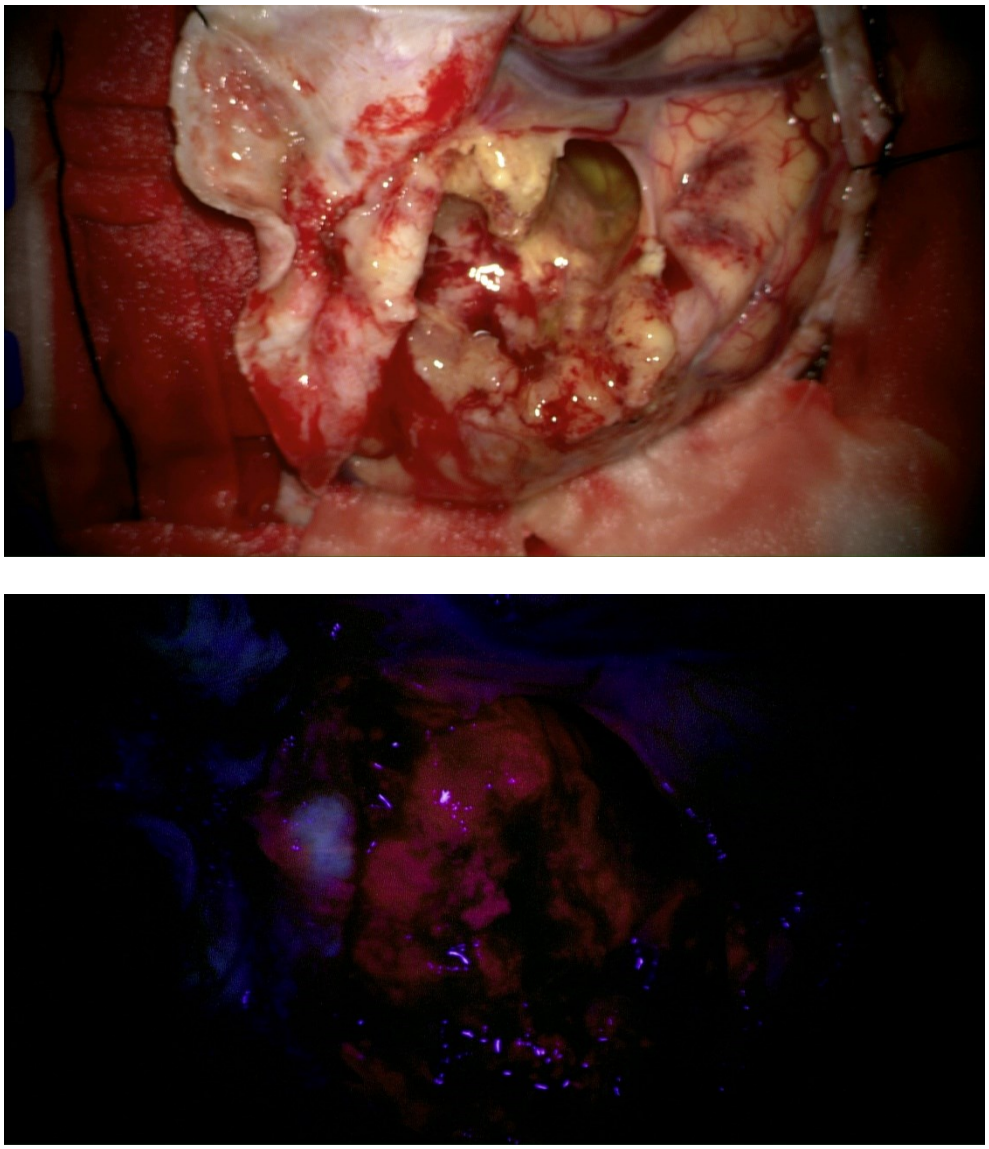

Figure 2B. Surgical view of left sided mass. Relatively hard textured mass was easily separated from the normal brain which also showed red fluorescence

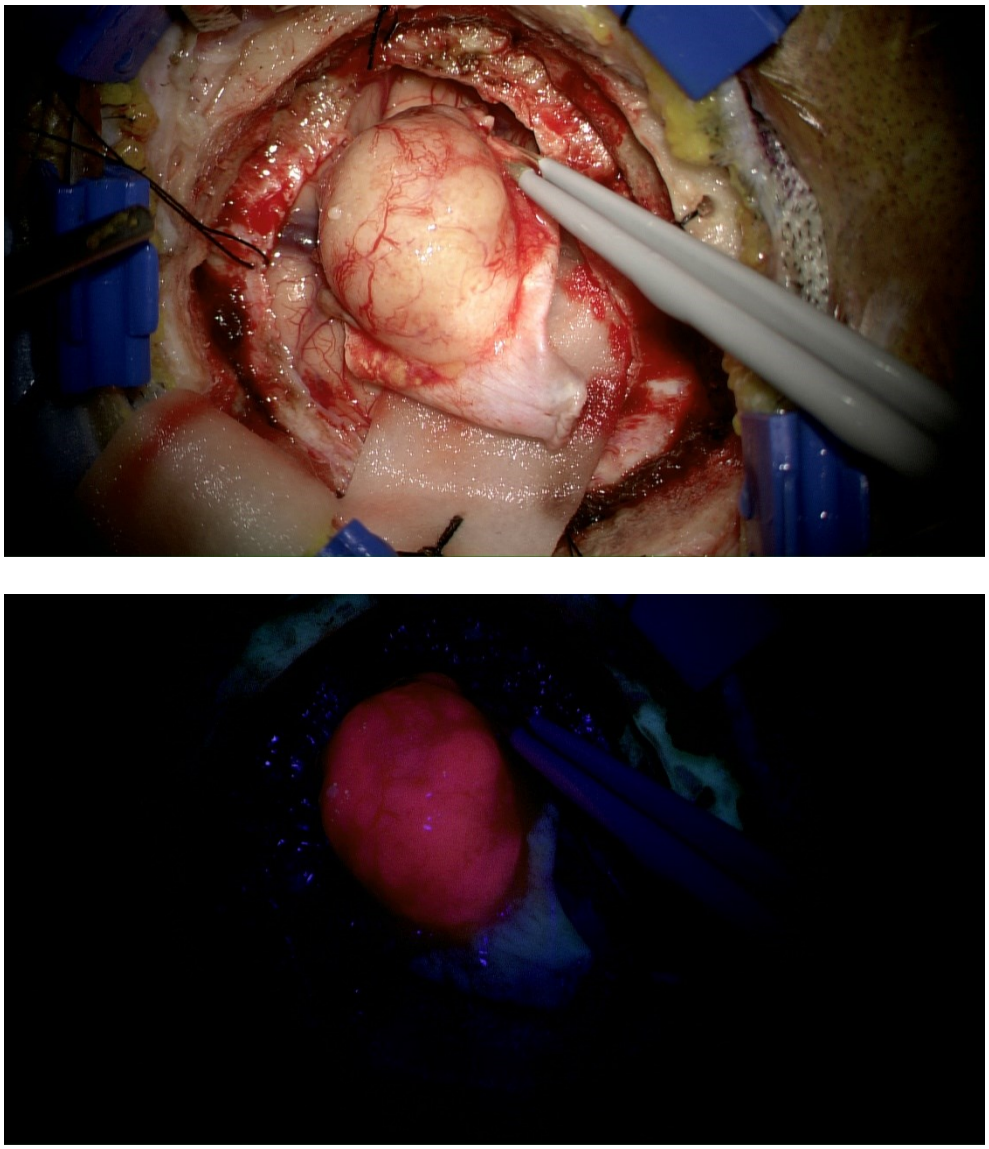

Figure 3A. Histological finding of atypical meningioma of meningothelial type (right sided tumor) showing increased mitotic figures of 4−10 mitosis/HPF (H&E staining, x200).

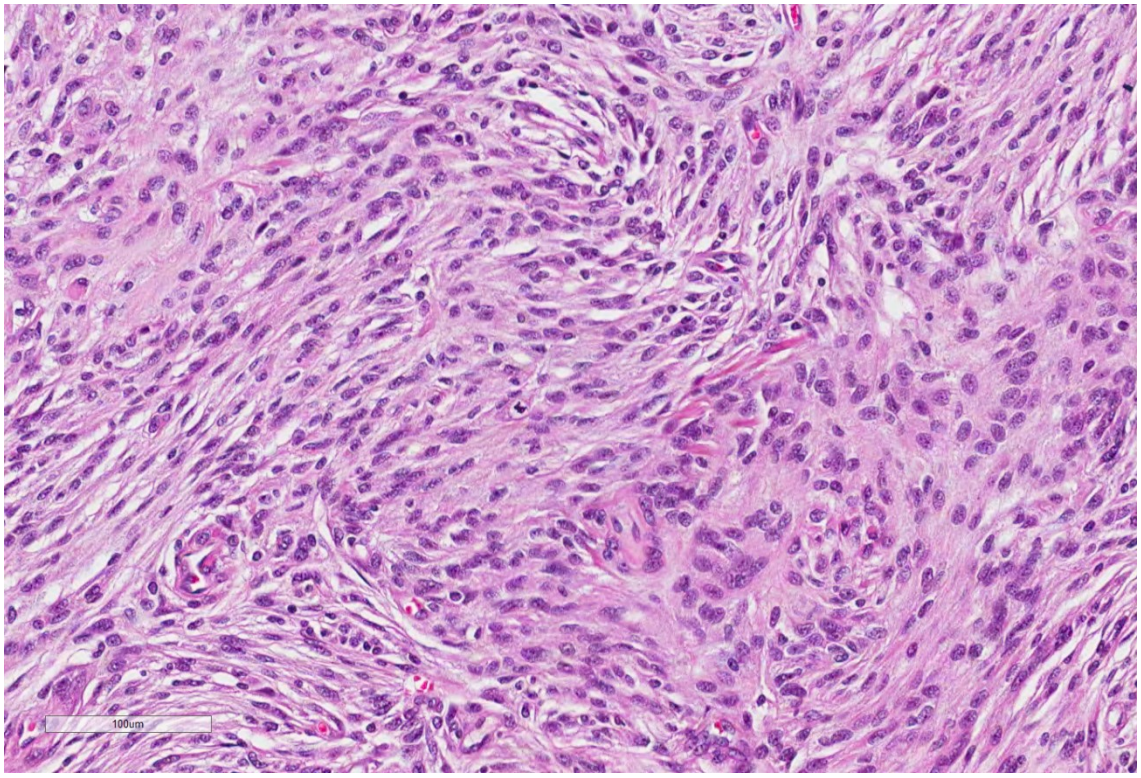

Figure 3B. Histological finding of benign meningioma of psammomatous type (left sided tumor) showing calcification, psammoma bodies and no mitosis (H&E staining x100).

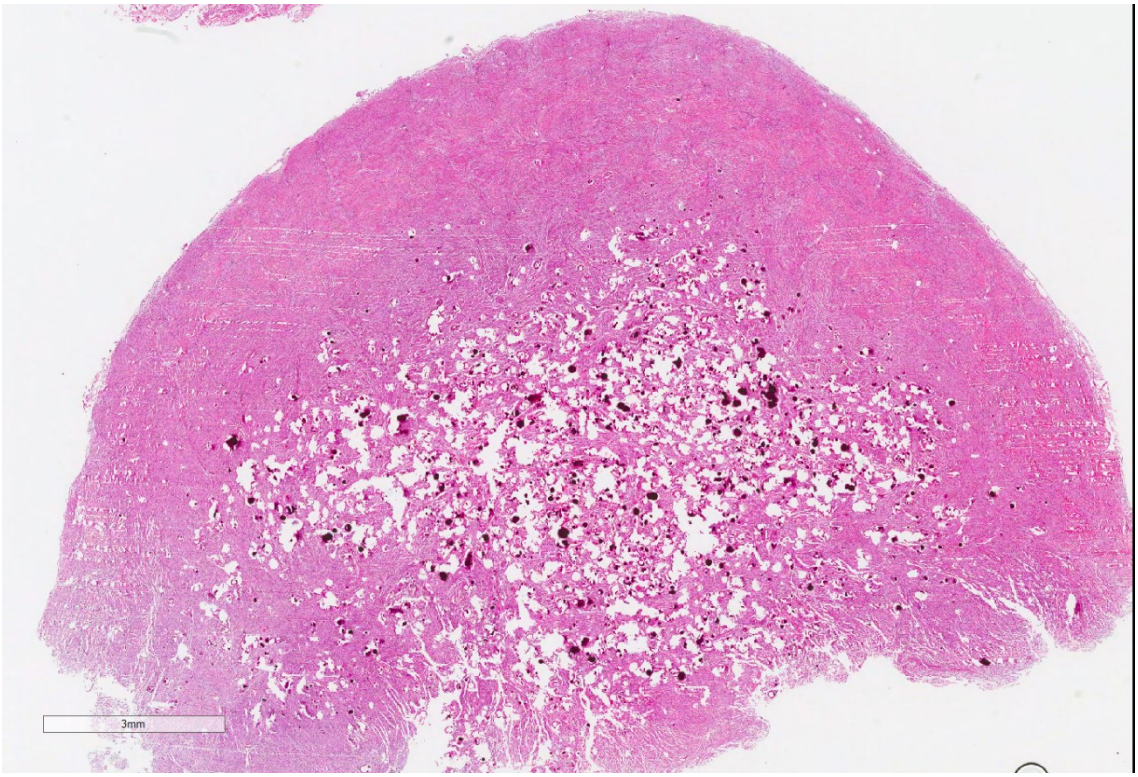

2.2 Sample Collection

Just after the resection, the samples were preserved in liquid nitrogen and then transferred to −80°C freezer. The written consent was taken from the patient according to the Institutional Review Board guidelines before tumor removal. Whole blood sample was also collected at the same time. From the whole blood sample, WBC buffy coat was extracted by centrifugation. The WBC was also preserved in −80°C freezer.

Genomic DNA was extracted using the QIAamp DNA mini kit (Qiagen, Valencia, CA, USA, Cat. No. 51304), and total RNA was extracted using RNeasy Plus Universal Mini Kit (Qiagen, Valencia, CA, USA, Cat. No. 73404) according to the manufacturer's recommendations. DNA content was quantitated using the Qubit DNA quantification Kit (Invitrogen, Carlsbad, CA, USA), and DNA integrity was assessed by gel electrophoresis. Samples with a RIN (RNA Integrity Number) > 5 were selected for the study.

2.3 Whole Exome Sequencing

Whole exome sequencing (WES) was performed at Macrogen, Inc. (Seoul, Korea). The SureSelectXT Library Prep Kit with SureSelectXT Target Enrichment System for Illumina Version B.2 protocol (Agilent Technologies, Santa Clara, CA, USA) was used for whole exome capture with 101−bp paired−end reads. The sequencer and sequencing control software were HiSEq 2000 sequencing system and HiSeq Control Software v2.2 (HCS, Illumina Inc., San Diego, CA, USA). The raw FASTQ files were obtained after sequencing.

2.4 RNA Sequencing

RNA sequencing (RNA-seq) library construction was performed using the TrueSeq Standard mRNA LT Sample Prep Kit following TruSeq Standard mRNA Sample Preparation Guide, Part # 15031047 Rev. E (Illumina Inc., San Diego, CA, USA). The sequencing was performed under the same platform used in WES.

2.5 Processing of Sequenced Data

For the generation of raw data from WES and RNA-seq, the Illumina Hiseq generates raw images utilizing HCS for system control and base calling through an integrated primary analysis software of RTA (Real Time Analysis. V1.18). The BCL (base calls) binary is converted into FASTQ utilizing illumine package bcl2fastq (v1.8.4).

For each tumor and control WBC sample 2 FASTQ files were generated. The FASTQ files were then further analyzed. At first, all the FASTQ files were aligned with a reference genome (UCSC Hg19) then corresponding FASTQ files for AMNG, BMNG and control were merged with each other. Alignment and merging were done by the Burrow Wheeler Alignment (BWA) software.[12, 13] After merging a sequence alignment/map (SAM) file is generated for each sample. These SAM files were then converted into binary alignment/map (BAM) files. The BAM files were then sorted by chromosome and PCR duplicates arising from the previous merging step were removed. SAM to BAM conversion, sorting and PCR duplicate removal were done by SamTools.[14] After that the BAM files were used for plotting the somatic calling, copy number variation calling and loss of heterozygosity calling using

an in-house Perl script described previously.[15] Genetic variants were annotated using the Yale N bulldog server. Variants were confirmed for true or false calling using Perl plotting and the false calling variants were sorted out.

To find out the top significant SNP variants the generated SNP calling file was further filtered for only AA to AB type missense, nonsense or exon in boundary mutation which were novel according to NHLBI and 1000 genome database, and arranged by ascending Fisher P value.

Differential gene expression was calculated from the RNA sequencing FASTQ files using the TOPHAT mapping program.[16] The genes with more than 4 log FC values were counted as upregulated. The circos diagram and differential gene graphs were plotted using R.[17, 18] PANTHER gene ontology and pathway analysis was used to functionally characterize differentially expressed genes.[19]

Additionally, the upregulated gene list for both AMNG and BMNG were further analyzed using the ToppGene Suit (http://toppgene.cchmc.org) for related pathways.[20] Pathways related to Biosystems: KEGG were chosen as the database. The cut off P value was 0.05.

Significant gene IDs of the SNP variants were also entered into GeneMANIA software (ver. 3.1.2.8, http://www.genemania.org) for network analysis.[21] Only the pathway option was chosen to specifically find out the pathways related to the significant genes.

Chapter 3. Results

3.1 Quality Control Assessment and Tumor Purity analysis

The raw data statistics of WES and RNA-seq are summarized in Table 1. All the generated data were acceptable for the analysis. Tumor purity was determined from the difference in allele frequencies of heterozygous SNPs in regions of loss of heterozygosity (LOH) in matched tumor and normal samples. Tumor purity analysis results were acceptable for both the tumors.

Table 1. Quality analysis of raw data from whole exome sequencing (WES) and RNA-sequencing (RNA-seq)

Parameters	Meningioma Grade I(BMNG)	Meningioma Grade II(AMNG)	Control (WBC)
WES			
Total Reads	171,702,816	174,467,322	142,211,318
GC(%)	45.057	48.103	47.736
AT(%)	54.94	51.9	52.26
Q20(%)	97.543	97.271	97.312
Q30(%)	95.933	95.422	95.566
Mean coverage depth (X)	178.193	206.8	175.9
Quantity of reads in total reads (all inside) (M)	58.7(46.88%)	68.4(41.5%)	58.0(43.3%)
Quantity of reads in total reads (allowing any overlap) (M)	101.9(80.8%)	121.3(73.6%)	103.4(77.2%)
Quantity of estimated reads that fall into total reads based on base-coverage (M)	89.3(70.82%)	103.7(62.8%)	88.2(65.8%)
Enrichment score by base coverage	70.82%	62.83%	65.80%
Average read length (bp)	101	101	101
RNA-seq			
Total Reads	80,503,180	84,481,796	
GC(%)	52.12	52.05	
AT(%)	47.88	47.95	
Q20(%)	94.85	95.61	
Q30(%)	88.43	89.46	
Overall read mapping rate	59.50%	90.40%	
No. of reads before mapped	80503180(80M)	84481796(84M)	
Aligned pairs	22222543	36635507	
Multiple alignments	4595167	3028663	
Discordant alignments	1867294	3551146	
Concordant pair alignment rate	50.60%	78.30%	

.Total reads: Total number of reads. In illumine paired-end sequencing, read 1 and read2 are added
.GC(%): GC content
.AT(%): AT content
.Q20(%): Ratio of reads that phred quality score of over 20 (Base call accuracy 99%).
.Q30(%):Ratio of reads that phred quality score of over 30 (Base call accuracy 99.9%).

3.2 No common gene mutations between synchronous meningiomas

The landscape of genetic events in BMNG and AMNG are visualized in Circos plot (Figure 4). After initial SNP calling a total of 2932 and 702 SNP mutations are found in both of the BMNG and AMNG.

After filtering, the number of mutations was reduced to 1878 in BMNG and 234 in AMNG (Figure 5). It is interesting to note that initially, BMNG had remarkably more mutations than AMNG. However, after further evaluation by perl plotting, only 6 genes(*PPFIBP2, RNF31, CSNK1G2, ATP6AT1, NF2,* and *SMARCB1*) and 8 genes (*FANCE, MLIP, PEAR1, TCEB3B, ZNF619, ZBTB41, TRPT1*, and *MST1L*) with lowest Fisher P score in BMNG and AMNG were identified, respectively (Table 2). There were no common somatic mutations between BMNG and AMNG.

Figure 4. Circos diagram of meningiomas (A. benign meningioma, B. atypical meningioma). From outer to inner the circles represent copy number variation (gain in blue, loss in red), chromosome numbers, reference Hg19 chromosome ideogram, SNP mutation gene names, base changes, SNP mutation type (missense in blue, nonsense in red, ex in boundary black), location of mutation, Fisher P score (less than 10^{-4} =red, greater than 10^{-4} =black) consequently.

A.

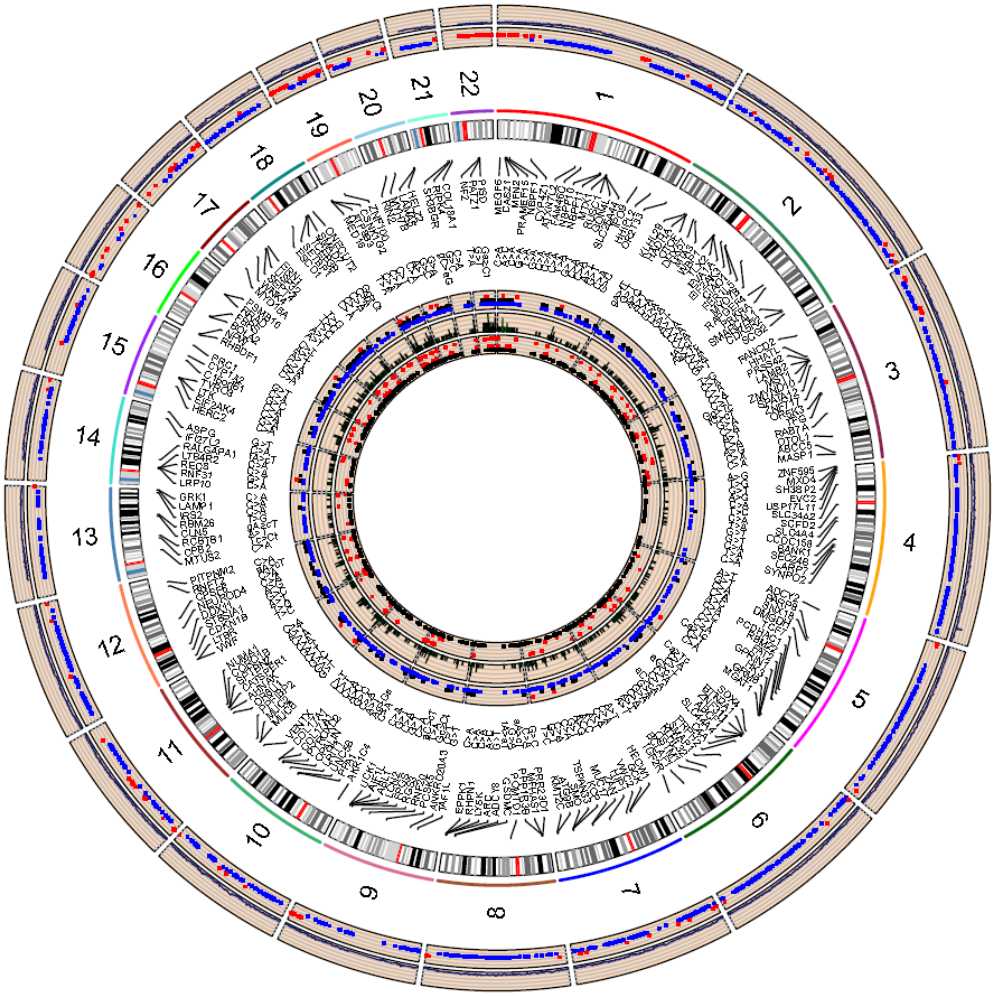

B.

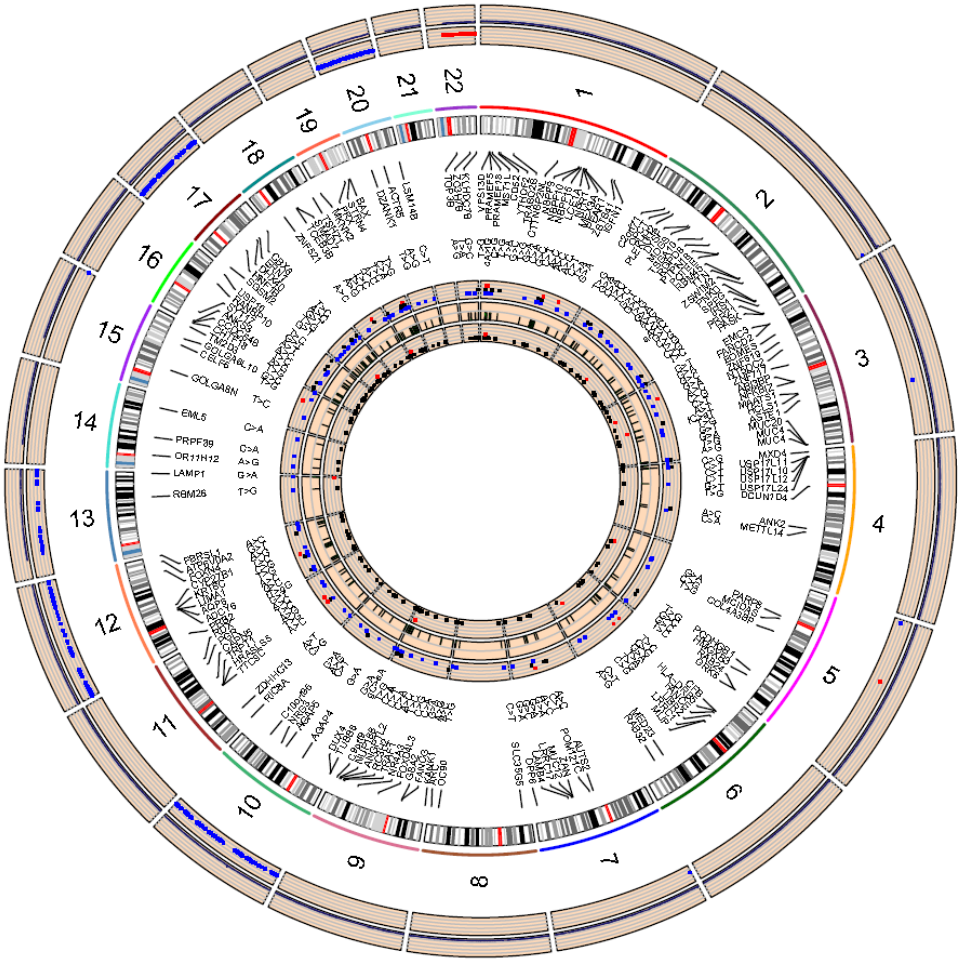
1
2
3
4
5
6
7
8
9
10
11
12
13
14
15
16
17
18
19
20
21
22
GOLGA8N T>C
EML5 C>A
PRPF39 C>A
OR11H12 A>G
LAMP1 G>A
RBM26 T>G

Figure 5. Number of SNP mutations in A. benign meningioma (BMNG) and B. atypical meningioma (AMNG) before and after filtering.

A.

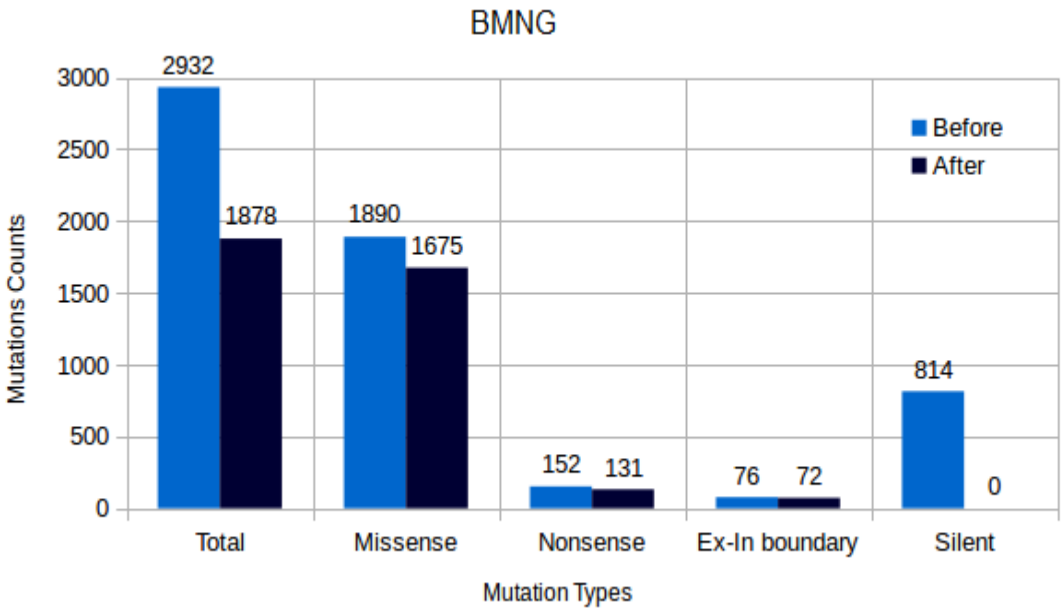

B.

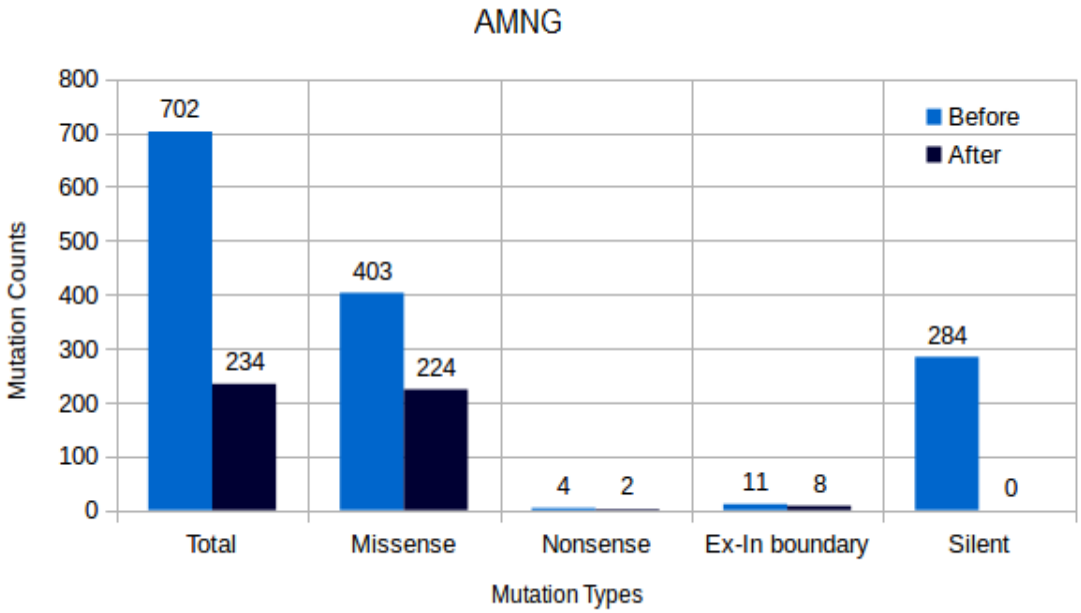

Table 2. Significant non-synonymous mutations.

Gene name	BMNG	AMNG	SNP mutation type	Fisher P	Chromosome	Position (hg19)	Base change	Mutation type	NHLBI%	1000 genomes
PEAR1	-	O	Missense	1.88E-29	Chr 1	156883040	C>T	AA>AB	Novel	Novel
ZBTB41	-	O	Missense	2.68E-16	Chr 1	197168723	T>A	AA>AB	Novel	Novel
MST1L	-	O	Exon in boundary	9.97E-04	Chr 1	17086183	T>G	AA>AB	Novel	Novel
ZNF619	-	O	Missense	1.67E-18	Chr 3	40528978	G>A	AA>AB	Novel	Novel
FANCE	-	O	Missense	2.64E-35	Chr 6	35427459	G>A	AA>AB	Novel	Novel
MLIP	-	O	Missense	1.22E-31	Chr 6	54122131	C>G	AA>AB	Novel	Novel
TRPT1	-	O	Missense	3.32E-08	Chr 11	63993323	A>G	AA>AB	Novel	Novel
TCEB3B	-	O	Missense	6.86E-21	Chr 18	44559972	A>G	AA>AB	Novel	Novel
PPFIBP2	O	-	Exon in boundary	2.73E-41	Chr 11	7656825	G>C	AA>AB	Novel	Novel
RNF31	O	-	Missense	4.95E-17	Chr 14	24618693	G>T	AA>AB	Novel	Novel
CSNK1G2	O	-	Missense	5.95E-04	Chr 19	1978937	C>A	AA>AB	Novel	Novel
NF2	O	-	Exon in boundary	5.29E-04	Chr 22	30070932	T>A	AA>AB	Novel	Novel
SMARCB1	O	-	Missense	2.00E-02	Chr 22	153663718	A>G	AA>AB	Novel	Novel
ATP6AP1	O	-	Missense	1.36E-04	Chr X	24175879	C>A	AA>AB	Novel	Novel

3.3. Common genetic event of Loss of heterozygosity in 22 in synchronous meningiomas

The number of copy number variants were also higher in BMNG than AMNG. Benign meningioma has copy number gains in large regions of all chromosomes except chromosome 16, 17, 19, 20, and 22, among which chromosome 22 harbors only copy number loss regions (Figure 4A). Otherwise, AMNG has copy number gains in focal regions of chromosomes 2, 3, 5, 7, 13, 15, and in almost all regions of chromosomes 10, 12, 17, and 20. Besides a focal region of chromosome 5, chromosome 22 harbors the only copy number loss regions in AMNG as well (Figure 4B). Chromosome 22 copy number loss and loss of heterozygosity (LOH) of chromosome 22 were the only shared genetic events of synchronous BMNG and AMNG (Figure 6). The AMNG shows additional LOH of chromosome 3.

Figure 6. Copy number alterations in chromosome 22 (A), and loss of heterozygosity profiling in chromosomes (B).

A.

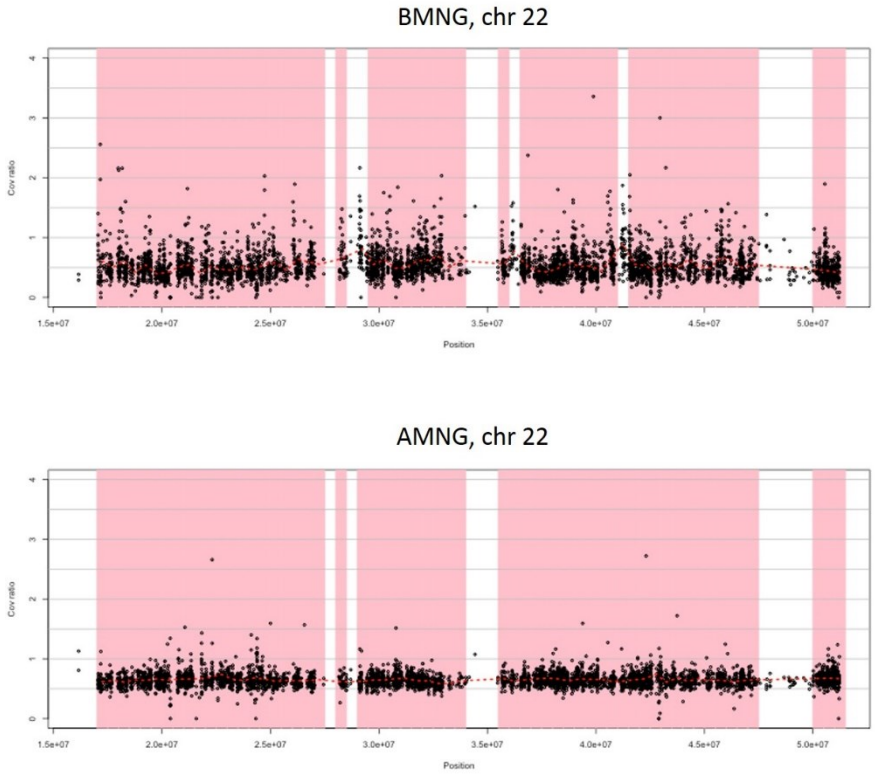

B.

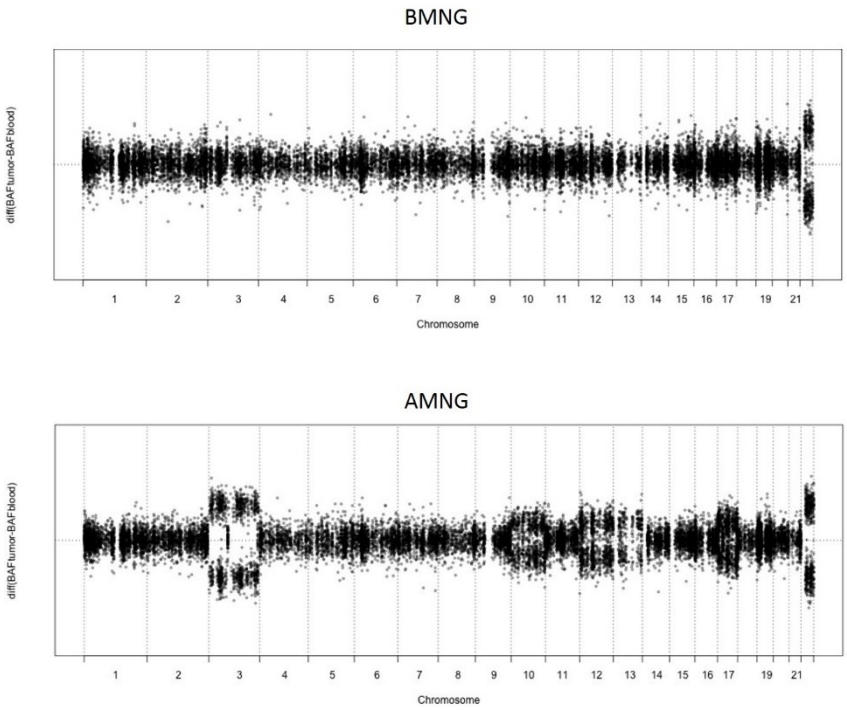

3.4 Differential gene expression analysis

In differential gene expression analysis between BMNG and AMNG, BMNG showed more upregulated genes than AMNG (log2 fold change >4), which corresponds to 789 and 255 respectively. (Fig 7). The list of 255 genes that were significantly overexpressed in AMNG compared to BMNG are listed in Table 3. Gene list analysis with those 255 overexpressed genes in AMNG successfully annotates 245 genes for 46 categories from PANTHER Classification system (http://www.pantherdb.org/). Among them, 12 gene categories are listed in Table 4 with more than 3 genes enriched to greater than 3.0% of gene hit against total numbers of pathway. It is notable that Integrin signaling pathway and Wnt signaling pathway are activated in AMNG. Additional analysis of differentially expressed genes using ToppGene suite revealed additional activation of Hedgehog pathway in AMNG (Table 5).

Figure 7. RNA sequencing differential gene expression showing up regulated genes in both Atypical and Benign meningioma. (Tumor 1 = Atypical, Tumor 2 = Benign)

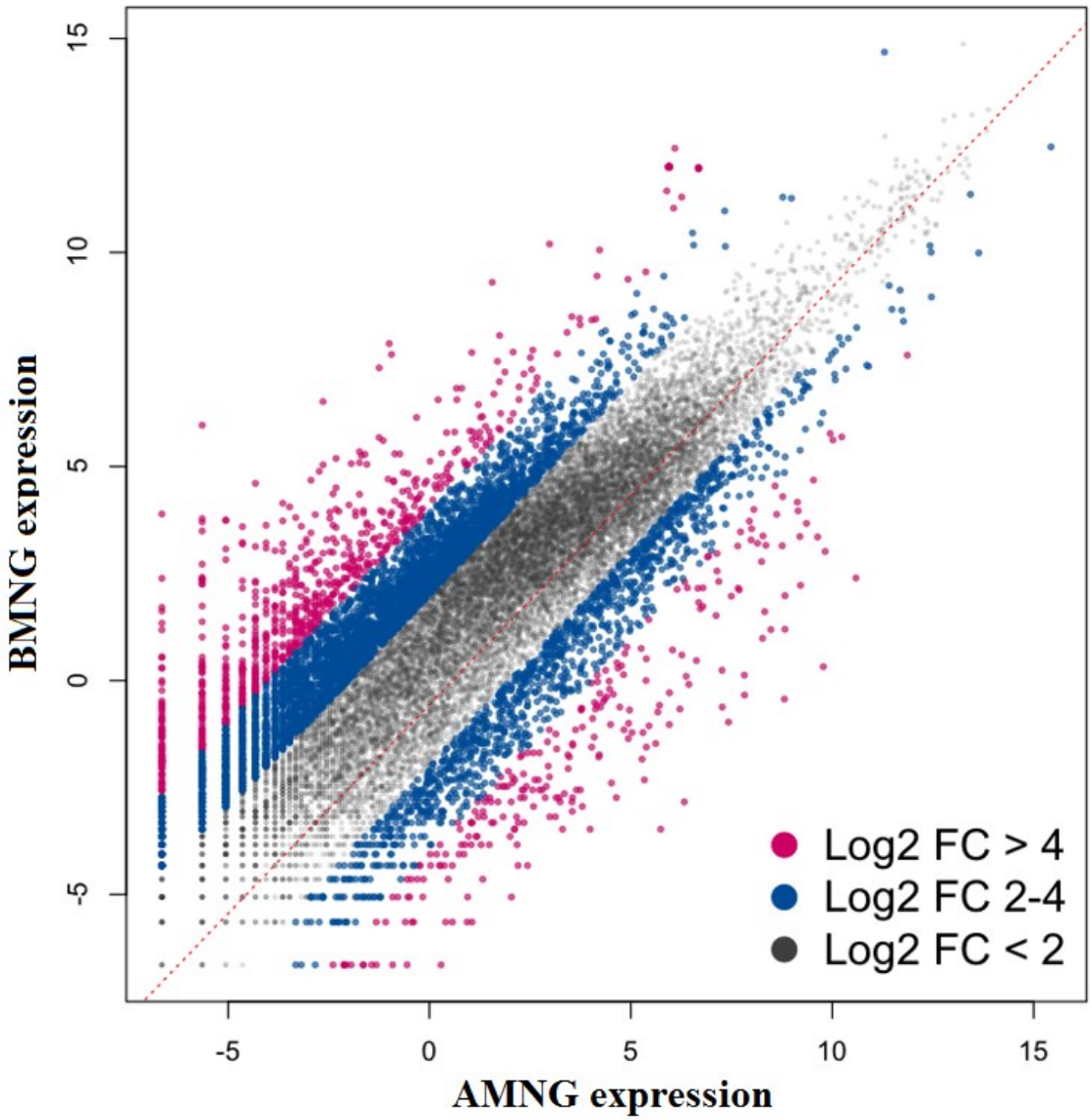

Table 3. Genes that are significantly overexpressed (log 2 fold change >4) in atypical meningioma compared to benign meningioma.

No	Gene	FPKM			log2 FC
		normal	AMNG	BMNG	
1	*IGHG1*	9.23	879.04	1.25	9.46
2	*C19orf33*	0.32	449.8	0.74	9.25
3	*TREM1*	1.21	53.46	0.09	9.21
4	*IGHA2*	0.02	80.21	0.14	9.16
5	*TPSAB1*	0	171.82	0.51	8.40
6	*IGKC*	13.6	1539.76	5.26	8.19
7	*IGHG2*	3.05	226.57	0.79	8.16
8	*IGHG3*	0.93	154.17	0.65	7.89
9	*IGHA1*	2.22	225.6	1.09	7.69
10	*PRAP1*	0.04	40.37	0.2	7.66
11	*IGLC2*	2.62	453.92	2.29	7.63
12	*MLPH*	0.17	15.88	0.09	7.46
13	*IGHM*	0.12	24.93	0.15	7.38
14	*IGLC3*	7.29	356.11	2.28	7.29
15	*TPSB2*	0.16	308.29	1.98	7.28
16	*CXCL1*	2.43	38.78	0.28	7.11
17	*NEFM*	430.21	4.1	0.03	7.09
18	*CA9*	0.42	49.05	0.36	7.09
19	*RP11-496I9.1*	0.06	153.59	1.18	7.02
20	*GDF15*	0.09	593.04	4.67	6.99
21	*PVALB*	111.6	62	0.49	6.98
22	*IL8*	4.82	41.74	0.34	6.94
23	*ADAMTS5*	0.17	1.22	0.01	6.93
24	*RP11-216L13.19*	0.37	22.92	0.19	6.91
25	*PPP1R1B*	104.54	74.37	0.63	6.88
26	*IGLC1*	1.45	454.14	3.95	6.85
27	*KRT18*	1.81	906.25	8.08	6.81
28	*SULT1E1*	0.04	9.87	0.09	6.78
29	*CBLN4*	6.84	5.4	0.05	6.75
30	*NEFL*	272.03	13.88	0.13	6.74
31	*PLA2G2A*	0.51	320.01	3.05	6.71
32	*RP11-809N8.2*	0	2.08	0.02	6.70
33	*LL22NC03-N14H11.1*	2.71	11.66	0.12	6.60
34	*F2RL1*	0.59	1.91	0.02	6.58

35	*ANGPTL4*	15.97	86.79	0.94	6.53
36	*LAG3*	0.35	4.59	0.05	6.52
37	*IGHD*	0.01	39.36	0.43	6.52
38	*PHLDA1*	9.61	43.7	0.48	6.51
39	*AC096579.7*	0.54	50.88	0.6	6.41
40	*ARHGEF16*	0.33	11.6	0.14	6.37
41	*APLN*	10.62	8.73	0.11	6.31
42	*CHRDL2*	0.21	13.41	0.17	6.30
43	*SLCO4A1*	5.48	30.64	0.39	6.30
44	*NXPH4*	1.07	52.36	0.67	6.29
45	*LAMA1*	0.83	11.71	0.15	6.29
46	*IFITM1*	41.4	796.56	10.22	6.28
47	*MT3*	377.85	82.84	1.07	6.27
48	*DHRS2*	0.44	32.62	0.43	6.25
49	*KRT14*	0.04	62.18	0.82	6.24
50	*NTSR1*	0.13	1.48	0.02	6.21
51	*GCGR*	0	12.53	0.17	6.20
52	*ATP2A1*	0.48	7.92	0.11	6.17
53	*STRA6*	0.21	98.89	1.38	6.16
54	*DNAH7*	0.93	0.68	0.01	6.09
55	*STC1*	0.85	9.47	0.14	6.08
56	*IGSF1*	2.53	1.32	0.02	6.04
57	*DHRS13*	2.64	4.52	0.07	6.01
58	*SALL1*	8.11	1.93	0.03	6.01
59	*RP11-352D13.5*	0	10.17	0.16	5.99
60	*SLC22A8*	0.94	18.4	0.29	5.99
61	*EGLN3*	15.87	28.41	0.45	5.98
62	*P2RX5*	3.33	2.5	0.04	5.97
63	*MZB1*	0.31	9.31	0.15	5.96
64	*OCIAD2*	32.91	18.6	0.3	5.95
65	*ANKRD1*	0.05	30.8	0.5	5.94
66	*TFPI2*	0.15	8.84	0.15	5.88
67	*SLC2A3*	29.24	586.83	10.3	5.83
68	*COBL*	20.86	0.53	0.01	5.73
69	*PDLIM1*	12.33	657.33	12.72	5.69
70	*VTN*	0.26	76.91	1.51	5.67
71	*RP11-60L3.1*	0	5.08	0.1	5.67
72	*SERPINE1*	1.86	31.29	0.62	5.66
73	*IL4I1*	0.66	4.01	0.08	5.65
74	*SERPINA3*	167.73	433.04	8.86	5.61
75	*ST14*	0.23	7.32	0.15	5.61
76	*C2*	2.13	138.72	2.86	5.60

77	*TK1*	0.59	4.33	0.09	5.59
78	*IGKV1-5*	0.42	16.3	0.34	5.58
79	*SDS*	4.11	4.31	0.09	5.58
80	*RBP1*	31.5	206.94	4.34	5.58
81	*CA8*	6.73	5.99	0.13	5.53
82	*RP11-742B18.1*	0	4.6	0.1	5.52
83	*COL18A1*	5.66	180.28	3.92	5.52
84	*NNAT*	33.35	22.52	0.49	5.52
85	*COL7A1*	0.65	202.72	4.46	5.51
86	*PAMR1*	14.17	10.87	0.24	5.50
87	*PLIN2*	8.53	303.17	6.86	5.47
88	*RP11-806H10.4*	0	17.03	0.4	5.41
89	*BOP1*	7.11	7.47	0.18	5.38
90	*KRT7*	0.13	41.47	1	5.37
91	*ETV4*	0.34	6.98	0.17	5.36
92	*CH25H*	3.07	4.48	0.11	5.35
93	*ECEL1*	0.1	26.46	0.65	5.35
94	*EPHA1*	0.37	2.8	0.07	5.32
95	*FBN3*	0.51	0.4	0.01	5.32
96	*AKR1C1*	4.24	65.53	1.64	5.32
97	*FGF17*	0.82	6.65	0.17	5.29
98	*MTRNR2L13*	0	11.09	0.29	5.26
99	*TRIM34*	0.91	0.76	0.02	5.25
100	*WNT4*	0.66	7.88	0.21	5.23
101	*FZD10*	0.21	0.74	0.02	5.21
102	*LRP2*	13.64	0.37	0.01	5.21
103	*HSPA6*	0.96	326.68	8.93	5.19
104	*ITGB4*	16.41	568.68	15.6	5.19
105	*SMTNL2*	0.7	10.82	0.3	5.17
106	*AQP9*	0.54	2.43	0.07	5.12
107	*CST7*	0.62	5.9	0.17	5.12
108	*ATG9B*	1.59	1.38	0.04	5.11
109	*PYY*	0.25	5.1	0.15	5.09
110	*IGLV2-8*	0.13	11.77	0.35	5.07
111	*DUSP5*	3.49	110.67	3.32	5.06
112	*UPP1*	8.07	105.86	3.2	5.05
113	*PROSER2-AS1*	0.28	0.66	0.02	5.04
114	*MYO1G*	1.91	6.52	0.2	5.03
115	*C11orf35*	0.08	11.71	0.36	5.02
116	*HSD17B2*	0	3.55	0.11	5.01
117	*AJAP1*	5.04	0.32	0.01	5.00
118	*INSRR*	0	0.32	0.01	5.00

119	*SERPINA5*	1.33	4.79	0.15	5.00
120	*SPP1*	669.62	562.08	17.96	4.97
121	*GRB14*	2.3	7.72	0.25	4.95
122	*CES1*	2.31	16.57	0.54	4.94
123	*IGFBP3*	15.85	283.06	9.23	4.94
124	*BMP6*	1.7	6.13	0.2	4.94
125	*AFAP1-AS1*	0.2	3.02	0.1	4.92
126	*RP1-179N16.6*	0.24	1.81	0.06	4.91
127	*CPXM1*	0.18	310.88	10.39	4.90
128	*TCAP*	0.63	5.07	0.17	4.90
129	*CHGB*	88.63	0.89	0.03	4.89
130	*PPP4R4*	10.11	1.48	0.05	4.89
131	*OLAH*	0.33	13.91	0.47	4.89
132	*CXCL2*	1.04	23.64	0.8	4.89
133	*ASPHD1*	34.62	5.3	0.18	4.88
134	*TESC*	11.9	41.68	1.42	4.88
135	*CYP2D6*	0.31	2.05	0.07	4.87
136	*OPTN*	60.03	145.24	4.97	4.87
137	*BTF3L4P2*	63.46	18.97	0.65	4.87
138	*AC092143.1*	0	4.08	0.14	4.87
139	*ARC*	1.56	2.91	0.1	4.86
140	*WNT6*	0.01	102.9	3.54	4.86
141	*MISP*	0.13	4.92	0.17	4.86
142	*PLTP*	34	741.85	25.67	4.85
143	*MIAT*	18.44	2.27	0.08	4.83
144	*LCN12*	1.66	19.84	0.71	4.80
145	*RP11-439E19.3*	0.83	2.23	0.08	4.80
146	*CYP2W1*	0.01	1.66	0.06	4.79
147	*FAM20A*	1.04	17.38	0.63	4.79
148	*EEF1A2*	186.72	20.4	0.74	4.78
149	*SLC16A6*	2.22	12.34	0.45	4.78
150	*IGLV1-51*	0.65	21.08	0.77	4.77
151	*ASGR1*	2.39	8.93	0.33	4.76
152	*HSPA1B*	73.24	393.3	14.73	4.74
153	*KRT17*	0.67	17.77	0.67	4.73
154	*HLA-G*	0.95	1.85	0.07	4.72
155	*FER1L4*	0.58	253.66	9.73	4.70
156	*KIAA1211*	2.5	0.26	0.01	4.70
157	*L1CAM*	22.98	1.29	0.05	4.69
158	*SLC6A12*	6.82	28.24	1.1	4.68
159	*MTFP1*	2.08	22.16	0.87	4.67
160	*SLC6A13*	3.03	110.85	4.48	4.63

161	*FXYD2*	0.15	1.73	0.07	4.63
162	*TUBB3*	121.94	17.17	0.7	4.62
163	*CNTD2*	0.1	1.96	0.08	4.61
164	*AL603965.1*	0	1.21	0.05	4.60
165	*MKI67*	0.05	0.24	0.01	4.58
166	*SPAG4*	0.96	140.78	5.89	4.58
167	*LY9*	0.03	1.19	0.05	4.57
168	*MEX3A*	0.28	0.71	0.03	4.56
169	*C1orf64*	1.13	0.47	0.02	4.55
170	*COL9A3*	17.83	1205.35	51.67	4.54
171	*ZMYND10*	2.38	2.56	0.11	4.54
172	*SLC5A5*	0.58	3.25	0.14	4.54
173	*F10*	0.47	18.74	0.81	4.53
174	*TRIM59*	8.93	0.23	0.01	4.52
175	*AC008132.13*	0.3	0.23	0.01	4.52
176	*OTOA*	0.09	0.69	0.03	4.52
177	*CAMK4*	7.98	0.23	0.01	4.52
178	*MSMP*	0.16	5.04	0.22	4.52
179	*FABP4*	2.75	201.32	8.83	4.51
180	*USH1C*	25.21	101.32	4.45	4.51
181	*REEP2*	44.52	38.21	1.68	4.51
182	*KLHDC7A*	0.01	0.9	0.04	4.49
183	*ADAM8*	0.17	22.02	0.99	4.48
184	*ETFB*	55.4	436.74	19.65	4.47
185	*RAB33A*	19.66	1.32	0.06	4.46
186	*IGHGP*	0.14	4.17	0.19	4.46
187	*ELF3*	0.53	13.58	0.62	4.45
188	*LAMA5*	2.43	255.54	11.69	4.45
189	*VSIG2*	0.17	4.34	0.2	4.44
190	*STC2*	0.93	13.67	0.63	4.44
191	*GPRC5A*	0.36	27.28	1.27	4.42
192	*RELL2*	9.77	6.65	0.31	4.42
193	*RPS14P3*	0.08	13.72	0.64	4.42
194	*RP11-196G11.1*	0.06	3.83	0.18	4.41
195	*OTOG*	0.02	2.32	0.11	4.40
196	*CFB*	4.03	1035.38	49.14	4.40
197	*MT1G*	43.24	25.67	1.22	4.40
198	*IL1R2*	0.24	8.8	0.42	4.39
199	*CDH10*	5.83	2.51	0.12	4.39
200	*LINC00202-2*	0.06	2.09	0.1	4.39
201	*DRD4*	0.31	7.62	0.37	4.36
202	*C19orf26*	1.42	2.88	0.14	4.36

203	*LINC00176*	0.24	2.05	0.1	4.36
204	*SRPX2*	0.7	2.05	0.1	4.36
205	*C16orf59*	0.59	1.02	0.05	4.35
206	*PLK5*	0.51	0.81	0.04	4.34
207	*ISM2*	0.27	3.64	0.18	4.34
208	*DPP4*	1.01	0.4	0.02	4.32
209	*ADM5*	0.13	4.16	0.21	4.31
210	*KISS1R*	0.03	3.5	0.18	4.28
211	*ADM2*	0.03	0.58	0.03	4.27
212	*CCL4L1*	4.63	5.98	0.31	4.27
213	*APOE*	296.16	3730.32	193.96	4.27
214	*MTRNR2L3*	0.53	211.38	11.11	4.25
215	*ALS2CR11*	0.32	0.19	0.01	4.25
216	*IGLON5*	4.09	25.18	1.33	4.24
217	*WFDC2*	2.83	84.64	4.48	4.24
218	*C2orf62*	0.53	1.13	0.06	4.24
219	*RARRES1*	0.79	2.82	0.15	4.23
220	*TCF15*	0.05	1.69	0.09	4.23
221	*MAFF*	7.15	28.89	1.55	4.22
222	*HBA2*	65.74	245.92	13.2	4.22
223	*GSTO2*	2.71	2.6	0.14	4.22
224	*CLDN5*	10.37	18.05	0.98	4.20
225	*ALPK2*	0.02	0.73	0.04	4.19
226	*HOXD9*	0	2.19	0.12	4.19
227	*HSPA1A*	28.75	987.98	54.57	4.18
228	*PIANP*	19.41	3.25	0.18	4.17
229	*HES4*	1.19	140.66	7.82	4.17
230	*IGFALS*	0.12	0.53	0.03	4.14
231	*PRKCZ*	62.61	20.69	1.18	4.13
232	*DNAAF3*	0.28	2.63	0.15	4.13
233	*RP11-392P7.6*	0.28	7.87	0.45	4.13
234	*PDIA2*	8.18	5.4	0.31	4.12
235	*ARL4C*	15.94	29.86	1.72	4.12
236	*LTF*	1.1	1.2	0.07	4.10
237	*C2CD4A*	0.1	0.68	0.04	4.09
238	*LIPH*	0.31	0.85	0.05	4.09
239	*TNFSF9*	3.49	16.29	0.96	4.08
240	*ESM1*	0.29	3.89	0.23	4.08
241	*RP11-365O16.6*	0.05	1.01	0.06	4.07
242	*FEZF1-AS1*	0.01	0.84	0.05	4.07
243	*TNXB*	3.02	265.53	15.95	4.06
244	*RP11-211G23.2*	0	4.78	0.29	4.04

245	*BCL2A1*	7.09	17.96	1.09	4.04
246	*PSMC1P5*	0	80.8	4.92	4.04
247	*ENO2*	362.91	382.75	23.36	4.03
248	*SAA1*	0.62	4.91	0.3	4.03
249	*DHDH*	0.83	2.29	0.14	4.03
250	*LRRC46*	0.61	1.63	0.1	4.03
251	*ACHE*	4.36	43.6	2.68	4.02
252	*PRMT8*	13.59	3.41	0.21	4.02
253	*VEGFA*	7.37	121.78	7.5	4.02
254	*PFKP*	85.36	119.7	7.38	4.02
255	*CHI3L2*	7	70.86	4.37	4.02

Table 4. The result of annotation of overexpressed genes in AMNG compared to BMNG using PANTHER classification system (http://www.pantherdb.org/).

Category name (Accession)	# of genes	percent of gene hit against total # of genes	percent of gene hit against total # of pathway	Genes
Integrin signalling pathway (P00034)	5	2.00%	5.50%	*LAMA5, LAMA1, ITGB4, COL9A3, COL18A1*
Wnt signaling pathway (P00057)	5	2.00%	5.50%	*PRKCZ, CDH10, FZD10, WNT6, WNT4*
CCKR signaling map (P06959)	5	2.00%	5.50%	*CXCL1, CXCL2, Serpine1, CAMK4, IL8*
Apoptosis signaling pathway (P00006)	4	1.60%	4.40%	*HSPA6, BCL2A1, HSPA1B, HSPA1A*
Alzheimer disease-presenilin pathway (P00004)	4	1.60%	4.40%	*FZD10, WNT6, WNT4, LRP2*
Inflammation mediated by chemokine and cytokine signaling pathway (P00031)	4	1.60%	4.40%	*PRKCZ, CCL4L1, CCL4L1, IL8*
Huntington disease (P00029)	4	1.60%	4.40%	*ARL4C, OPTN, DNAH7, TUBB3*
Cadherin signaling pathway (P00012)	4	1.60%	4.40%	*CDH10, FZD10, WNT6, WNT4*
Angiogenesis (P00005)	3	1.20%	3.30%	*PRKCZ, GRB14, VEGFA*
Parkinson disease (P00049)	3	1.20%	3.30%	*HSPA6, HSPA1B, HSPA1A*
Nicotinic acetylcholine receptor signaling pathway (P00044)	3	1.20%	3.30%	*MYO1G, ACHE, ACHE*
Gonadotropin-releasing hormone receptor pathway (P06664)	3	1.20%	3.30%	*PRKCZ, HSPA1B, BMP6*

Table 5. Network analysis of differentially expressed genes between BMNG and AMNG using ToppGene suite.

Pathway Term	KEGG pathway number	BMNG	AMNG	Count	%	P value	Adjusted P value (Benjamini)	Genes
Neuroactive ligand−receptor interaction	hsa04080	O	−	15	0.47	0.0001	0.01	*F2RL2, CCKAR, PTGER3, LEPR, ADCYAP1R1, LHCGR, VIPR1, P2RY13, GRM4, PRLR, P2RY2, P2RY14, GLP2R, TSHR, GHR*
Cytokine−cytokine receptor interaction	hsa04060	O	−	15	0.47	0.0001	0.01	*TNFSF4, LEPR, CXCL9, TGFB3, CCL19, PF4, CNTFR, KIT, CXCL10, CCL25, PRLR, CXCL14, CX3CR1, TPO, GHR*
Chemokine signaling pathway	hsa04062	O	−	10	0.32	0.0047	0.14	*CCL25, CXCL14, CX3CR1, CXCL9, CCL19, JAK2, PF4, GNB4, PIK3R1, CXCL10*
Jak−STAT signaling pathway	hsa04630	O	−	7	0.22	0.0509	0.71	*PRLR, LEPR, TPO, CNTFR, JAK2, PIK3R1, GHR*
Ribosome	hsa03010	O	−	5	0.16	0.0631	0.71	*RPL7AP30, RPS27P29, RPSAP15, RPL7P26, RPL31P49, RPS27P23*
Dilated cardiomyopathy	hsa05414	O	−	5	0.16	0.0743	0.70	*ACTC1, ITGA8, PLN, TGFB3, IGF1*
Calcium signaling pathway	hsa04020	O	−	7	0.22	0.0832	0.69	*CCKAR, PTGER3, PDE1C, PLN, RYR3, LHCGR, MYLK*
Glycine, serine and threonine metabolism	hsa00260	O	−	3	0.09	0.0997	0.71	*MAOA, BHMT, DAO*
ECM−receptor interaction	hsa04512	−	O	6	0.30	0.006	0.43	*LAMA1, TNXB, LAMA5, ITGB4, VTN, SPP1*
Complement and coagulation cascades	hsa04610	−	O	5	0.25	0.015	0.51	*F10, CFB, SERPINA5, SERPINE1, C2*
Hedgehog signaling pathway	hsa04340	−	O	4	0.20	0.043	0.74	*WNT4, LRP2, WNT6, BMP6*
Focal adhesion	hsa04510	−	O	7	0.35	0.060	0.77	*LAMA1, TNXB, LAMA5, VEGFA, ITGB4, VTN, SPP1*
Pathways in cancer	hsa05200	−	O	9	0.45	0.085	0.81	*LAMA1, WNT4, FZD10, IL8, LAMA5, FGF17, VEGFA, EGLN3, WNT6*

3.5 Hypothesis of genomic evolution process of meningioma development and progression

The GeneMANIA pathway analysis of the top SNP variants of BMNG and AMNG showed different pathway network relations of each tumor. Among the six significant mutated genes of AMNG mentioned in Table 2, only *SMARCB1* gene was present in different pathway network with significant FDR value. From the eight AMNG genes only the *FANCE* and *MST1L* genes were present in different FDR significant pathway. The pathway names and FDR values are shown in Table 6. Therefore, this again confirms that there is no shared genetic events and process regarding meningiomagenesis except for LOH of chromosome 22. And, it is postulated that multiple additional mutations in each tumor contribute to the further development of tumors. It is unlikely that the primary tumor cell or precursor cells may spread to different areas and make a daughter tumor. A schematic diagram of this process is showed in Figure 8. Considering all the genetic data together, it is plausible that accumulation of LOH, rather than specific de novo mutation is responsible for the progression of meningioma to a higher grade. However, it is interesting to implicate the Fanconi anemia pathway component mutation (*FANCE*) for the activation of Wnt and Hedgehog pathway in AMNG. Disruption in the Fanconi anemia DNA repair system may impact on meningioma progression into higher grade by involving Wnt and Hedgehog signaling pathways.

Table 6. Pathways related to non-synonymous SNP mutations (http://genemania.org)

Pathway Function	BMNG	AMNG	FDR value	SNP variants present in network
rRNA transcription	-	O	3.325e-12	*MST1L*
Fanconi anaemia nuclear complex	-	O	1.651e-10	*FANCE*
transcription from RNA polymerase III promoter	-	O	1.736e-10	*MST1L*
nuclear transcription factor complex	-	O	0.000003	*MST1L*
transcription factor complex	-	O	0.001044	*MST1L*
npBAF complex	O	-	0.002620	*SMARCB1*
nBAF complex	O	-	0.002991	*SMARCB1*
SWI/SNF complex	O	-	0.005393	*SMARCB1*
nucleosome disassembly	O	-	0.006424	*SMARCB1*
chromatin disassembly	O	-	0.006424	*SMARCB1*
BAF-type complex	O	-	0.006424	*SMARCB1*
protein-DNA complex disassembly	O	-	0.006424	*SMARCB1*

Figure 8. Schematic diagram of development and progression of synchronous different graded meningioma in this study

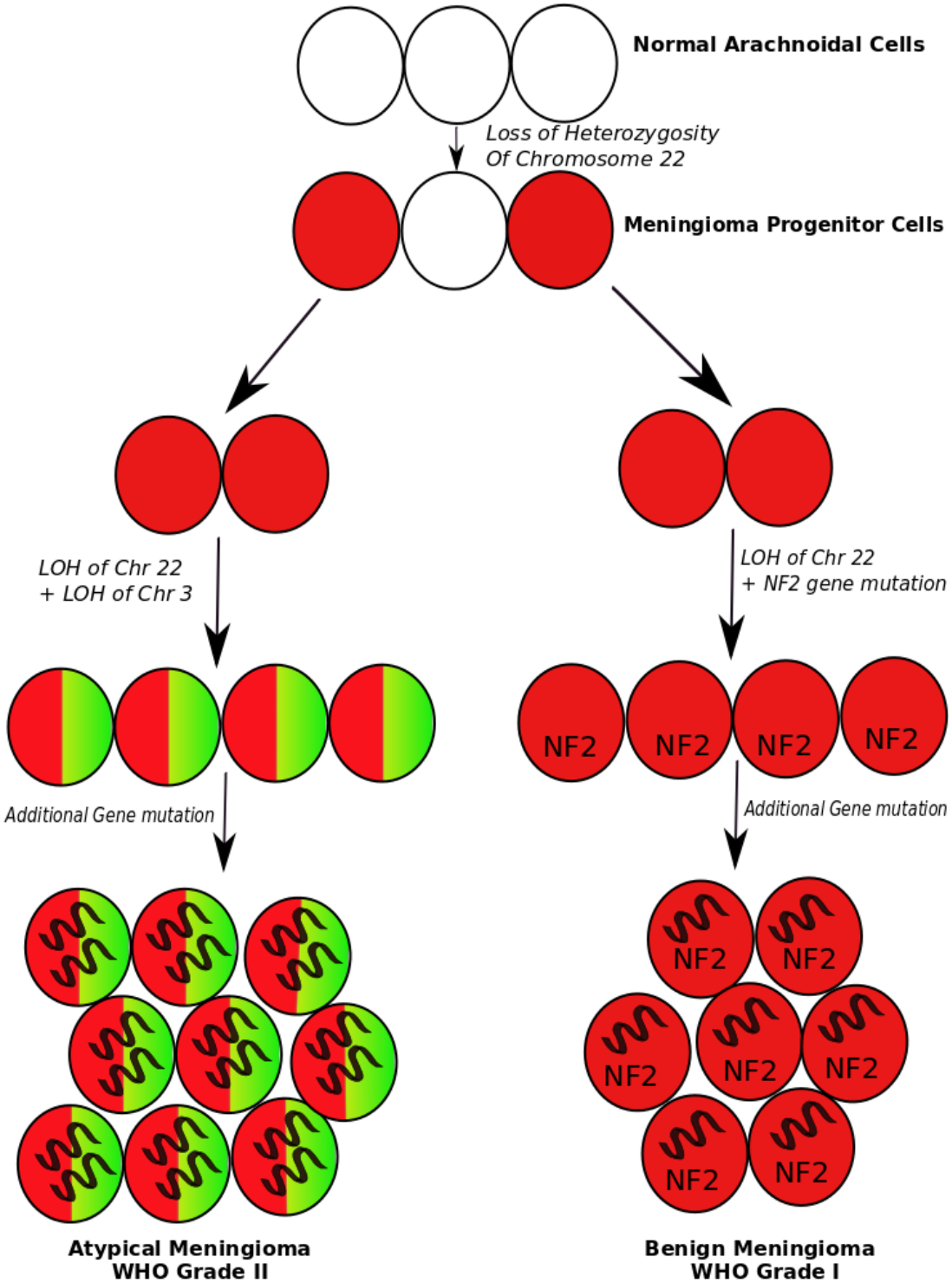

Chapter 4. Discussion

In the present genomic profiling of synchronous meningiomas of different histological grade, two tumors harbor distinct genomic signatures. Although chromosome 22 LOH was the only common genetic event in both tumors, no shared mutations were found. This suggests that there were no common founder events involving de novo somatic driver mutations for the origin of these synchronous bilateral meningiomas. However, both tumors had an only shared genomic event of LOH of chromosome 22. This implies that this may be the initial stimulation to transform normal arachnoid cap cells into meningioma precursor cells. The LOH of chromosome 22 is the most common genetic event in meningioma described in the previous studies.[8, 22-25] At least 60% of the meningioma harbors the chromosome 22 loss.[26] Other common LOH in meningioma reported in various studies are of chromosome 1, 10 and 14.[25, 27] *SMARCB1*, which was found in the BMNG of the present study, is also reported previously in some cases of multiple meningiomas.[28, 29] But the role of *SMARCB1* mutation in the development of the multiple meningiomas in the present case is not clear due to its presence in only BMNG.

Earlier genetic studies in both solitary and multiple meningioma cases have shown that meningioma development is complex and often due to multiple genetic events playing equal roles.[30, 31]

According to previous studies development of a meningioma can be explained by a four-hit mechanism.[28] If we apply the present case into the four-hit mechanism hypothesis, the loss of the chromosome 22 can be consi

dered as the first hit in the process of development of the multiple mening ioma (Figure 8). Previous studies on synchronous meningiomas of different grade suggested that independent progression process could be the cause of the different histopathological and karyotypic features.[32-34] Past ge netic study on synchronous lung adenocarcinoma has also revealed that sy nchronous tumor development can be driven by distinct molecular events si milar to our study results.[35] Similarly, the present case of no shared mu tations between BMNG and AMNG support the hypothesis of an independe nt genomic process for the progression of these tumors. In a previous syn chronous colorectal carcinoma mutation profile study on a Lynch patient sh owed that synchronous tumor can follow highly distinct oncogenic pathway s for development and progression.[36] So the presence of versatile mutat ions in synchronous tumors is not uncommon.

The AMNG is reported to show much more versatile genetic mutations co mpared to the BMNG.[25] In the present case, AMNG showed additional L OH of chromosome 3 in addition to chromosome 22. LOH of multiple chro mosomes is previously reported in higher grades of meningioma such as th e atypical and anaplastic meningioma.[6] In an earlier basic research of col orectal cancer high LOH status had been associated with higher grade of c arcinoma.[37] We could also identify accumulation of additional LOH of chr omosome 3 in AMNG in the present case. Hence, it is thought that comple xity of LOH, rather than the accumulation of point mutations, is more impo rtant for the meningioma progression into a higher grade.

In the pathway analysis by PANTHER and ToppGene, we found functional relation of differential genes of AMNG with the Wnt signaling pathway and the

Hedgehog pathway. Some recent gene expression studies have linked both the Wnt signaling pathway and the hedgehog pathways to meningioma development and progression.[38-41] Some of them found that these pathways were more related with the higher grade meningiomas (e.g. atypical, anaplastic) than the lower grade meningiomas.[42, 43] Also in a medulloblastoma study, aberrant SNP mutations and multiple LOH events were stated as the main cause for the Wnt pathway activation.[44]

Another significant fact is both of these pathways have been showed to have cross-linkage with each other in different cancer studies which found that activation of either one of the pathway sometimes leads to activation of the other.[45-47]

Among the genes that are related to the Wnt and Hedgehog pathways in our study, two genes (*WNT4* and *WNT6*) were present in both. So it is possible that in the AMNG the Wnt and Hedgehog pathways might be cross-linked with each other via these two genes.

Among the pathways related to the SNP mutations, it is noticeable that the involvement of Fanconi anemia pathway in AMNG. This pathway has been mentioned to have common genetic susceptibility with breast cancer and brain tumors.[48] This is a very compelling finding because in some previous studies it was suggested that the Fanconi anemia pathway and the Wnt signaling pathway might share some common effectors.[49, 50]

Comparing all these previous findings with our data we could contemplate that, in the AMNG, the *FANCE* gene mutation activated the Fanconi Anemia pathway which combined with the multiple LOH leads to the activation of Wnt signaling pathway. Then the Hedgehog pathway was activated through

the cross-linking with the Wnt pathway and all these interlinked events played a role in development and progression of AMNG in this patient. But more future large-scale studies are needed to validate the relation of Fanconi anemia pathway, Wnt Signalling and Hedgehog pathways with AMNG progression.

Chapter 5. Conclusion

It can be concluded from this study that synchronous meningioma of different grades can be progressed independently due to separate genetic mutation and pathways even after originating from a single common genetic event, in this case, LOH of chromosome 22. Also higher grade meningiomas may have an association with accumulation of LOH events. Large-scale genetic studies of a specific region of interest of could be helpful in future studies to identify specific driver genes for meningioma. It is also evident that the development and progression of meningioma is a complex process which is driven by multiple genetic events and pathways. Our study provides scopes for many future researches to understand the molecular mechanism behind development and progression of meningioma.

Bibliography

1. *Meningioma - Statistics*. Cancer.Net 2012 2012/06/25/T23:52:28-04:00 2016/07/15/03:59:50; Available from: http://www.cancer.net/cancer-types/meningioma/statistics files/21/statistics.html.
2. Lee, C.-H., et al., *Epidemiology of primary brain and central nervous system tumors in Korea.* Journal of Korean Neurosurgical Society, 2010. **48**(2): p. 145-152.
3. Jung, K.-W., et al., *An Updated Nationwide Epidemiology of Primary Brain Tumors in Republic of Korea.* Brain Tumor Research and Treatment, 2013. **1**(1): p. 16-23.
4. Louis, D.N., et al., *The 2016 World Health Organization Classification of Tumors of the Central Nervous System: a summary.* Acta Neuropathologica, 2016. **131**(6): p. 803-820.
5. Zang, K.D., *Meningioma: a cytogenetic model of a complex benign human tumor, including data on 394 karyotyped cases.* Cytogenet Cell Genet, 2001. **93**(3-4): p. 207-20.
6. Sandberg, A.A. and J.F. Stone, *The Genetics and Molecular Biology of Neural Tumors*. 2008: Springer Science & Business Media. 453.
7. Brastianos, P.K., et al., *Genomic sequencing of meningiomas identifies oncogenic SMO and AKT1 mutations.* Nature genetics, 2013. **45**(3): p. 285-289.
8. Clark, V.E., et al., *Genomic analysis of non-NF2 meningiomas reveals mutations in TRAF7, KLF4, AKT1, and SMO.* Science (New York, N.Y.), 2013. **339**(6123): p. 1077-1080.
9. Jacoby, L.B., et al., *Clonal analysis of human meningiomas and schwannomas.* Cancer Res, 1990. **50**(21): p. 6783-6.
10. Zhu, J., et al., *Analysis of meningiomas by methylation- and transcription-based clonality assays.* Cancer Res, 1995. **55**(17): p. 3865-72.
11. van den Munckhof, P., et al., *Germline SMARCB1 mutation predisposes to multiple meningiomas and schwannomas with preferential location of cranial meningiomas at the falx cerebri.* Neurogenetics, 2012. **13**(1): p. 1-7.
12. Li, H. and R. Durbin, *Fast and accurate short read alignment with Burrows-Wheeler transform.* Bioinformatics (Oxford, England), 2009. **25**(14): p. 1754-1760.
13. Li, H., *A statistical framework for SNP calling, mutation discovery, association mapping and population genetical parameter estimation from sequencing data.* Bioinformatics (Oxford, England), 2011. **27**(21): p. 2987-2993.
14. Li, H., et al., *The Sequence Alignment/Map format and SAMtools.* Bioinformatics (Oxford, England), 2009. **25**(16): p. 2078-2079.
15. Choi, M., et al., *K+ Channel Mutations in Adrenal Aldosterone-Producing Adenomas and Hereditary Hypertension.* Science (New York, N.Y.), 2011. **331**(6018): p. 768-772.
16. Trapnell, C., L. Pachter, and S.L. Salzberg, *TopHat: discovering splice junctions with RNA-Seq.* Bioinformatics, 2009. **25**(9): p. 1105-1111.
17. Team, R.C., *R: A Language and Environment for Statistical Computing*. 2013, R Foundation for Statistical Computing: Vienna, Austria.
18. Zhang, H., P. Meltzer, and S. Davis, *RCircos: an R package for Circos 2D track plots.* BMC Bioinformatics, 2013. **14**: p. 244.
19. Thomas, P.D., et al., *PANTHER: a library of protein families and subfamilies indexed by function.* Genome Res, 2003. **13**(9): p. 2129-41.
20. Chen, J., et al., *ToppGene Suite for gene list enrichment analysis and candidate gene prioritization.* Nucleic Acids Res, 2009. **37**(Web Server issue): p. W305-11.
21. Warde-Farley, D., et al., *The GeneMANIA prediction server: biological network*

integration for gene prioritization and predicting gene function. Nucleic Acids Res, 2010. **38**(Web Server issue): p. W214-20.
22. Seizinger, B.R., et al., *Molecular genetic approach to human meningioma: loss of genes on chromosome 22.* Proceedings of the National Academy of Sciences of the United States of America, 1987. **84**(15): p. 5419-5423.
23. Ruttledge, M.H., et al., *Deletions on chromosome 22 in sporadic meningioma.* Genes, Chromosomes & Cancer, 1994. **10**(2): p. 122-130.
24. Akagi, K., et al., *Deletion mapping of the long arm of chromosome 22 in human meningiomas.* International Journal of Cancer, 1995. **60**(2): p. 178-182.
25. Chang, I.B., et al., *Loss of Heterozygosity at 1p, 7q, 17p, and 22q in Meningiomas.* Journal of Korean Neurosurgical Society, 2010. **48**(1): p. 14.
26. Meese, E., N. Blin, and K.D. Zang, *Loss of heterozygosity and the origin of meningioma.* Human Genetics, 1987. **77**(4): p. 349-351.
27. Mihaila, D., et al., *Meningiomas: analysis of loss of heterozygosity on chromosome 10 in tumor progression and the delineation of four regions of chromosomal deletion in common with other cancers.* Clinical Cancer Research: An Official Journal of the American Association for Cancer Research, 2003. **9**(12): p. 4435-4442.
28. Christiaans, I., et al., *Germline SMARCB1 mutation and somatic NF2 mutations in familial multiple meningiomas.* Journal of Medical Genetics, 2011. **48**(2): p. 93-97.
29. Torres-Martín, M., et al., *Whole exome sequencing in a case of sporadic multiple meningioma reveals shared NF2, FAM109B, and TPRXL mutations, together with unique SMARCB1 alterations in a subset of tumor nodules.* Cancer Genetics, 2015. **208**(6): p. 327-332.
30. Collins, V.P., M. Nordenskjold, and J.P. Dumanski, *Molecular Genetics of Meningioma.* Brain Pathology, 1990. **1**.
31. Simon, M., et al., *Allelic Losses on Chromosomes 14, 10, and 1 in Atypical and Malignant Meningiomas: A Genetic Model of Meningioma Progression.* Cancer Research, 1995.
32. Koh, Y.C., et al., *Multiple meningiomas of different pathological features: case report.* J Clin Neurosci, 2001. **8 Suppl 1**: p. 40-3.
33. Tomita, T., et al., *Multiple meningiomas consisting of fibrous meningioma and anaplastic meningioma.* Journal of Clinical Neuroscience, 2003. **10**(5): p. 622-624.
34. Yang, G., et al., *Multiple meningiomas characterized by benign and malignant tumor entities.* CNS Neurosci Ther, 2013. **19**(12): p. 984-6.
35. Liu, Y., et al., *Genomic heterogeneity of multiple synchronous lung cancer.* Nat Commun, 2016. **7**: p. 13200.
36. Wheeler, S.R., et al., *Mutation profiles of synchronous colorectal cancers from a patient with Lynch syndrome suggest distinct oncogenic pathways.* J Gastrointest Oncol, 2016. **7**(3): p. E64-71.
37. Chang, S.-C., et al., *Loss of heterozygosity: An independent prognostic factor of colorectal cancer.* World Journal of Gastroenterology, 2005.
38. Laurendeau, I., et al., *Gene expression profiling of the hedgehog signaling pathway in human meningiomas.* Mol Med, 2010. **16**(7-8): p. 262-70.
39. Bale, A.E., *Hedgehog signaling and human disease.* Annu Rev Genomics Hum Genet, 2002. **3**: p. 47-65.
40. Pecina-Slaus, N., A. Kafka, and M. Lechpammer, *Molecular Genetics of Intracranial Meningiomas with Emphasis on Canonical Wnt Signalling.* Cancers (Basel), 2016. **8**(7).
41. Mawrin, C. and A. Perry, *Pathological classification and molecular genetics of meningiomas.* J Neurooncol, 2010.
42. Ragel, B.T. and R.L. Jensen, *Aberrant signaling pathways in meningiomas.* J Neurooncol, 2010. **99**(3): p. 315-24.
43. Wrobel, G., et al., *Microarray-based gene expression profiling of benign,*

atypical and anaplastic meningiomas identifies novel genes associated with meningioma progression. Int J Cancer, 2005. **114**(2): p. 249-56.
44. Yokota, N., et al., *Role of Wnt pathway in medulloblastoma oncogenesis.* Int J Cancer, 2002. **101**(2): p. 198-201.
45. Song, L., et al., *Crosstalk between Wnt/beta-catenin and Hedgehog/Gli signaling pathways in colon cancer and implications for therapy.* Cancer Biol Ther, 2015. **16**(1): p. 1-7.
46. Taipale, J. and P.A. Beachy, *The Hedgehog and Wnt signalling pathways in cancer.* Nature, 2001. **411**.
47. Choy, W., et al., *The molecular genetics and tumor pathogenesis of meningiomas and the future directions of meningioma treatments.* Neurosurg Focus, 2011. **30**(5): p. E6.
48. Offit, K., et al., *Shared Genetic Susceptibility to Breast Cancer, Brain Tumors, and Fanconi Anemia.* JNCI Journal of the National Cancer Institute, 2003. **95**(20): p. 1548-1551.
49. Huard, C.C., et al., *The Fanconi anemia pathway has a dual function in Dickkopf-1 transcriptional repression.* Proc Natl Acad Sci U S A, 2014. **111**(6): p. 2152-7.
50. Huard, C.C., et al., *Fanconi anemia proteins interact with CtBP1 and modulate the expression of the Wnt antagonist Dickkopf-1* Blood, 2012.

Abstract in Korean

서로 다른 조직학적 단계의 동시성 뇌수막종의 유전체 변이 특성 비교

뇌수막종(Meningioma)은 중추신경계에서 흔히 발생하는 양성 종양이다. 최근 뇌수막종과 관련한 주요 변이들이 보고되고 있지만, 구체적인 변이를 확인하기 위한 보다 상세한 유전적 연구가 필요하다. 본 논문에서는 다중 수막종(multiple meningioma) 환자의 검체에서 조직학적으로 다른 악성도를 보이는 두 부위의 검체를 whole-exome study 하여 악성도에 따른 유전적 변이를 확인하기 위한 연구를 진행하였다. 실제 같은 환자라고 하더라도 악성도의 차이를 보이는 병변에서 변이가 상의함을 확인하였다. 발암개시(Tumor initiation)단계에서 22번 염색체의 이형접합성상실(loss of heterozygosity)이 공통적으로 나타나지만, 후속 변이가 뇌수막종의 악성도에 영향을 주는 것을 확인하였다.

중요단어: 뇌수막종, 다중 수막종, Whole exome study, 이형접합성상실

학번: 2015-22194